Available online at www.sciencedirect.com
SCIENCE DIRECT
Journal of Catalysis 242 (2006) 38–47
JOURNAL OF CATALYSIS
www.elsevier.com/locate/jcat

Catalytic removal of NO_x and diesel soot over nanostructured spinel-type oxides

D. Fino *, N. Russo, G. Saracco, V. Specchia

Department of Materials Science and Chemical Engineering, Politecnico di Torino, C.so Duca degli Abruzzi 24, 10129 Torino, Italy

Received 22 March 2006; revised 23 May 2006; accepted 25 May 2006

Available online 30 June 2006

Abstract

Nanostructured spinel-type oxide catalysts AB_2O_4 (where A = Co and Mn, and B = Cr and Fe), prepared by the solution combustion synthesis method and characterized by BET, XRD, FESEM, TEM, FTIR, and catalytic activity tests, proved to be effective in the simultaneous removal of soot and NO_x, the two prevalent pollutants in diesel exhaust gases in the temperature range of 350–450 °C. The activity order for soot combustion was found to be $CoCr_2O_4 > MnCr_2O_4 > CoFe_2O_4$, whereas the activity order for NO_x reduction was $CoFe_2O_4 > CoCr_2O_4 > MnCr_2O_4$. The best compromise between simultaneous abatement of soot and nitrogen oxide was therefore shown by $CoCr_2O_4$ catalyst; it could promote soot combustion and appreciable NO_x reduction below 400 °C, the maximum temperature reached in the exhaust line of a diesel engine. On the basis of oxygen temperature-programmed desorption, the prevalent catalytic combustion activity of the chromite catalysts could be explained by their higher concentration of suprafacial, weakly chemisorbed oxygen, which contributes actively to soot combustion by spillover in the temperature range of 300–500 °C. Tentative reaction pathways for the simultaneous reduction of NO_x are outlined as well.

Keywords: Diesel particulate combustion; Nitrogen oxides reduction; $CoCr_2O_4$; $MnCr_2O_4$; $CoFe_2O_4$ spinels; Reaction mechanism

1. Introduction

The increased industrialization, and particularly increased traffic, in Western and developing nations has been accompanied by a negative impact on air quality, the environment, and human health. Diesel engines have both carbon monoxide and unburned hydrocarbon outlet concentrations much lower than those produced by spark-ignition engines. However, even the most recent diesel engines (e.g., common rail) generate nitrogen oxides and carcinogenic particulates, whose size (50–200 nm) falls in the so-called lung-damaging range [1]. Many toxicologic and epidemiologic studies have established adverse health effects by particulate matter (PM10, PM2.5). There is increasing evidence that several health effects are associated with the ultrafine particles (diameter <100 nm) [2]. Recent research shows that these can penetrate the cell membranes, enter the blood, and even reach the brain [3]. Some investigations indicate that such particles can induce inheritable mutations [4].

The automotive industry is currently facing serious challenges to reduce the environmental impact from vehicles since European legislation introduced the Euro 4 step in January 2005, which for diesel cars corresponds to 0.25 g km^{-1} of NO_x and 0.025 g km^{-1} of particulate matter (PM). Despite an 80% reduction in diesel car emission standards over the levels of 10 years ago, the mean NO_x emission level of diesel vehicles continues to be three times higher than their gasoline counterparts.

These limits cannot be accomplished by engine modifications [5], fuel pretreatments [6], or simply better tuning of the combustion process [7]; thus, a convenient way of treating diesel off-gases is needed. In this context, a possible solution to reduce the PM emissions of vehicles is to retrofit them with a particulate filter. Several diesel particulate filter systems are currently on the market. Wall-flow monoliths are the most common type [8]. Adjacent channels in the wall-flow filters are alternatively plugged at each end, thus forcing the gas to flow through the porous wall, which acts as a filter medium. The most important issue with diesel traps is the regeneration of the

* Corresponding author. Fax: +39 011 5644699.
E-mail address: debora.fino@polito.it (D. Fino).

0021-9517/$ – see front matter
doi:10.1016/j.jcat.2006.05.023

filters. Various strategies for this have been considered, including catalyzed filter substrates [9–11], fuel-borne catalysts [12], continuous regenerating traps [13], electric heaters [14], fuel burners [15], and microwaves [16].

The research carried out worldwide in this field is aimed mainly at two different solutions:

1. Filtration of particulate in a first catalytic converter, in which the soot is trapped and burned out due to the presence of a catalyst thoroughly deposited onto the filter [17], with NO_x eliminated in a second catalytic converter either by reaction with suitable reducing agents (e.g., light hydrocarbons, fuel, ammonia [18]) or by direct decomposition [19].
2. Simultaneous removal of soot and nitrogen oxides in a single, suitably catalyzed trap [20–32].

The second approach is clearly more ambitious than the first one and has recently been explored in view of the considerable advantages that it may offer in terms of both investment cost and pressure drop reduction. It is well known that 10–15% of NO_x is generally reduced during regeneration of soot-laden traps. This reduction mostly involves NO_2 molecules by direct reaction with soot to form NO and, to a much lesser extent, N_2 and N_2O [33]. This reaction, exploited in Johnson Matthey's continuously regenerating technology (CRT) [34], is the basis of the present study. Despite the fact that several technical problems remain to be solved (e.g., determining the best catalyst deposition route on the trap and the best trap design so as to allow intimate contact between the reactants and the catalyst itself), a more urgent research topic is the development of a suitable catalyst capable of promoting both soot oxidation and NO_x reduction at comparatively low temperatures (possibly within the range typical of diesel exhaust, 150–380 °C). A recent paper [35] has shown that mixed-type oxides are among the most promising catalysts for this purpose.

In the present work, nanostructured AB_2O_4 (with A = Co and Mn, and B = Cr and Fe) spinel-type catalysts were prepared via a tailored technique (i.e., solution combustion synthesis [36]), characterized, and tested for their activity in the simultaneous abatement of NO_x and soot. The nanoscopic dimensions of the catalyst crystals thus obtained was pursued so as to increase the number of contact points between the catalyst and the particulate, a key feature of the reaction pathway, as discussed later. On the basis of the experimental work reported here, some conclusions are then drawn concerning the catalysts tested.

2. Experimental

2.1. Catalyst preparation

Three spinel samples ($CoCr_2O_4$, $MnCr_2O_4$, and $CoFe_2O_4$) were prepared via a highly exothermic and self-sustaining reaction, the so-called *solution combustion synthesis* (SCS) method [36]. This technique is particularly suitable for producing nanosized catalyst particles. The combustion synthesis process can be formally split into the following two steps (using the preparation of cobalt chromite as an example):

$$3Co(NO_3)_2 + 6Cr(NO_3)_3 \rightarrow 3CoCr_2O_4 + 12N_2 + 30O_2 \quad (1)$$

and

$$20CO(NH_2)_2 + 30O_2 \rightarrow 20CO_2 + 40H_2O + 20N_2. \quad (2)$$

The first step is the endothermic reaction (1) for the real spinel synthesis starting from the metal nitrate precursors, whereas the second step is exothermic and accounts for the reaction (2) between oxygen derived from nitrates decomposition and urea. Of course, some direct combustion of urea with atmospheric oxygen cannot be excluded, because the preparation is carried out in air in an electric oven maintained at 500 °C, hosting the precursor mixture placed in a porcelain pot. The overall set of reactions is markedly exothermic, which leads to a thermal peak in the reacting solid mixture greatly exceeding 1000 °C for a few seconds. To increase this sudden heat release, some NH_4NO_3 was used. Under these conditions, nucleation of spinel crystals was induced, the growth of these crystals was limited, and nanosized grains were obtained, as anticipated. Each preparation batch was tuned to produce 1 g of the desired catalyst. After preparation, all catalysts were ground in a ball mill at room temperature and submitted to physical and chemical characterization.

A sample of the fresh $CoCr_2O_4$ was aged for 1 h at 900 °C in an oven to induce a decrease in the specific surface area and to evaluate the effect of this parameter on the catalytic activity.

2.2. Catalyst characterization

Catalyst characterisation was carried out via the following techniques:

- Chemical analysis of the catalyst was performed by atomic absorption spectroscopy (AAS) in a Perkin-Elmer 1100B spectrophotometer after dissolution in strongly acidic media, to verify the amount of each constituting element in the prepared spinels.
- X-ray diffraction (XRD) was done in a PW1710 Philips diffractometer equipped with a CuK_α monochromator to confirm that the desired spinel crystal structure was actually achieved.
- Field-emission scanning electron microscopy (FESEM) with a Leo 50/50 VP with a GEMINI column and transmission electron microscopy (TEM) with a Philips CM 30 T were carried out to analyze the microstructure of the catalyst crystal agglomerates and the catalyst crystals themselves.
- Nitrogen adsorption for BET specific surface area (SSA) measurements were performed with a Micromeritics ASAP 2010.
- Temperature-programmed desorption (TPD) analyses were also performed on all of the prepared catalysts in a Thermoquest TPD/R/O 1100 analyzer, equipped with a thermal conductivity detector (TCD) and a quadrupole mass spectrometry (MS) detector (Baltzer Quadstar 422). A fixed

bed of catalyst was enclosed in a quartz tube and sandwiched between two quartz wool layers; before each TPD run, the catalyst was heated under an O_2 flow at a rate of 40 Nml min^{-1} up to 750 °C. After 30 min at this temperature as a common pretreatment, the reactor temperature was lowered to room temperature with the same flow rate of oxygen, thereby allowing complete oxygen adsorption over the catalyst. Afterward, helium was fed to the reactor at a rate of 10 Nml min^{-1}, and the reactor was maintained at room temperature for 1 h to purge any excess oxygen molecules. The catalyst was then heated to 1100 °C at a constant rate of 10 °C min^{-1} under a helium flow rate of 10 Nml min^{-1} [37]. The quadrupole detector confirmed that oxygen was the only desorbed species.

– Two Fourier transform infrared (FTIR) spectra were recorded to provide crucial information about the reaction mechanism over the most promising catalyst ($CoCr_2O_4$), pretreated as follows: (a) fresh catalyst, as prepared, and (b) catalyst treated at 385 °C under NO flow (2000 ppmv in He) for 60 min and then cooled rapidly under pure He gas flow, with the reactor then promptly removed from the oven. A 200-mg pellet was formed by pressing a mixture of each treated catalyst and KBr (1:100 weight ratio). FTIR transmission spectra were then obtained in the wavenumber range 1000–2000 cm^{-1} using a Bruker Equinox 55 spectrophotometer equipped with an MCT cryodetector.

2.3. Catalytic activity assessment

The catalytic activity of the prepared catalysts was tested in a temperature-programmed reaction (TPR) apparatus [38]. A standard gas mixture (1000 ppm NO, 10 vol% O_2, balance He) was fed at the constant flow rate of 1.66×10^{-6} $Nm^3\,s^{-1}$ via a set of mass flow meters (Brooks) to a fixed-bed reactor enclosed in a quartz tube placed in an electric oven. The tubular quartz reactor was loaded with 50 mg of a 9:1 by weight mixture of powdered catalyst and carbon and 150 mg of SiO_2 granules (0.3–0.7 mm); this inert material was added to reduce the specific pressure drops across the reactor and to prevent thermal runaways (maximum temperature difference across the reactor, 20 °C). The catalyst weight-to-flow rate ratio in the standard runs was $W/F = 27.1$ kg s Nm^{-3}. Experiments were performed by using instead of real diesel soot an amorphous carbon (printex U by Degussa) with the following properties: average particle size, 45 nm; 0.34 wt% ash after calcination at 800 °C; and 12.2 wt% of moisture lost after drying at 110 °C. This material was chosen to avoid any interference due to the presence of adsorbed HCs, sulfates, or fly ash present in real diesel soot. Moreover, the carbon used is more difficult to burn than diesel soot, making the results achieved conservative [9,39,40]. A proper and reproducible mixing between catalyst and carbon was routinely obtained by ball milling for 15 min. These mixing conditions are normally known as "tight contact" conditions [17] and were used in the present study because they allow for better reproducibility. The soot–catalyst contact conditions in a real catalytic trap are less intensive, however, and are usually referred to as "loose contact" conditions [17]. Similar conditions can be obtained by gently shaking the two counterparts in a vessel. Most runs in the present investigation were performed under tight contact conditions, because good reproducibility is mandatory to provide a sound basis for mechanistic studies. Reference runs on a loose contact mixture in the absence of catalyst (noncatalytic soot combustion) or the absence of soot (simple NO reduction by the catalyst) were also performed for comparison purposes.

The catalyst–carbon–SiO_2 fixed bed was sandwiched between two quartz-wool layers, whereas the tip of a K-type thermocouple was located well inside the bed itself. The reaction temperature was controlled through a PID-regulation system based on the measurements of an external K-type thermocouple and varied during each TPR runs from 200 to 700 °C at a rate of 5 °C min^{-1}. A 30-min stay at 200 °C under He flow was adopted as a common pretreatment to eliminate possible contaminants, such as adsorbed water. The analysis of the outlet gas was performed via a $CO/CO_2/N_2O$ NDIR analyzer, a NO/NO_2 chemiluminescence analyzer, and an O_2 paramagnetic analyzer by ABB. Nitrogen was measured by gas chromatography using a Hewlett Packard 5890 Series II, equipped with Porapak Q and molecular sieve columns and a TCD.

Specific TPR analyses were performed on the most promising catalyst prepared ($CoCr_2O_4$) for the sake of gaining better insight into the reaction mechanism:

(i) Runs at various inlet O_2 partial pressures (0, 2, 10 vol%; 1000 ppmv NO; balance He).
(ii) Runs at various inlet NO concentrations of (500, 1000, 2000 ppmv NO; 10 vol% O_2).
(iii) Runs at various catalyst/carbon ratios in the fixed bed (4:1, 9:1, 19:1, 1:0, being the amount of carbon equal to 5 mg, whenever present; at 1000 ppmv NO, 10 vol% O_2, balance He).

3. Results and discussion

All spinel catalyst samples were well crystallized by XRD analysis (Fig. 1). All diffraction peaks expected according to the reference JPCDS cards ($CoCr_2O_4$, PDF 221084; $CoFe_2O_4$, PDF 221086; $MnCr_2O_4$, PDF 751614) were observed. No secondary phases could be detected by this technique. XRD has a ±4% precision, and thus the presence of amorphous phases cannot be completely excluded. Moreover, chemical analysis (dissolution and atomic absorption, O_2 titration) confirmed, within the limits related to its intrinsic precision (±5%), that the amounts of the various constituting elements (Co, Cr, Fe, Mn, and O) were consistent with those used in the precursors and was compatible with the phases detected by XRD.

In the present context, spinel crystals with size of the same order of magnitude as that of the particulate nuclei (tens of nanometers [41]) are expected to provide the highest specific number of contact points between the soot directly captured over the catalyst layer of diesel particulate traps [42] and the crystals constituting such a layer. Fig. 2 shows a TEM picture of the $CoCr_2O_4$ spinel-type catalyst produced via SCS, which displays the highest SSA value (59.0 $m^2\,g^{-1}$). The spinel crys-

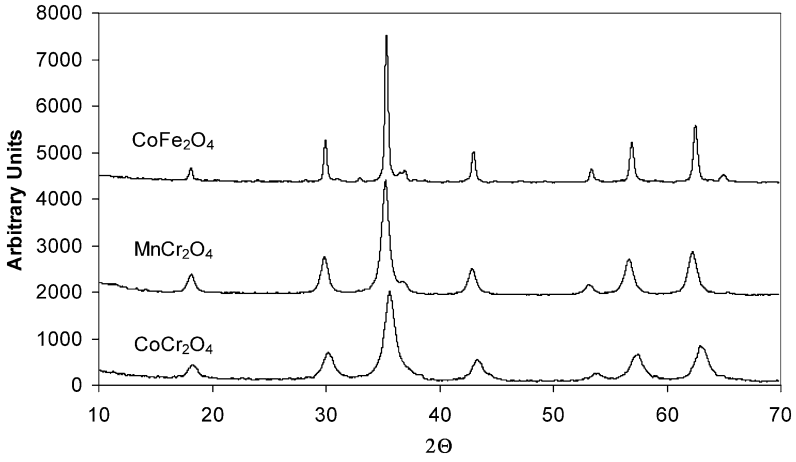

Fig. 1. XRD spectra of the three spinel-type catalysts prepared.

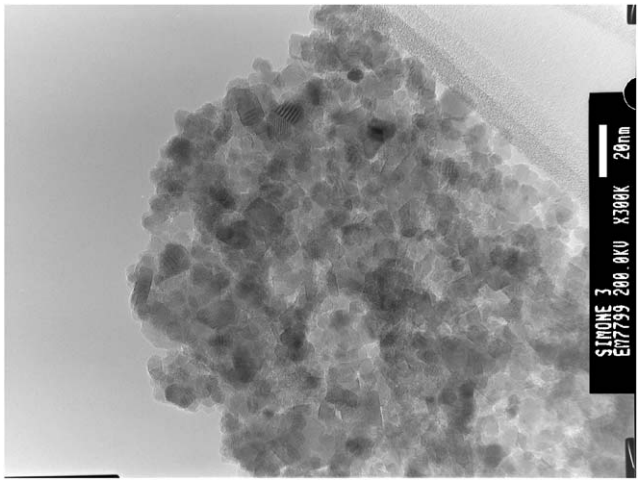

Fig. 2. TEM micrograph of the $CoCr_2O_4$ catalyst crystals.

tals of the considered catalyst are much smaller than 20 nm, perfectly in line with the dimensions of particulate nuclei and in substantial agreement with the SSA measured. As expected, this SSA was somehow reduced after calcination at high temperature (900 °C), even if it remains higher than that of the two other catalytic materials prepared.

The FESEM view of the microstructure of the crystal aggregates of the $CoCr_2O_4$ catalyst (Fig. 3) enlightens a very foamy structure, a typical feature of catalysts synthesized by SCS. This should once again strongly favor the contact between soot and catalyst even under loose contact conditions and, once coated on the wall flow trap channel walls, it should allow just a slight increase in the pressure drop [42].

Beyond the SSA data, Table 1 summarizes the carbon combustion peak temperatures (the temperature corresponding to the maximum carbon conversion rate to CO_2, T_{comb}), the maxi-

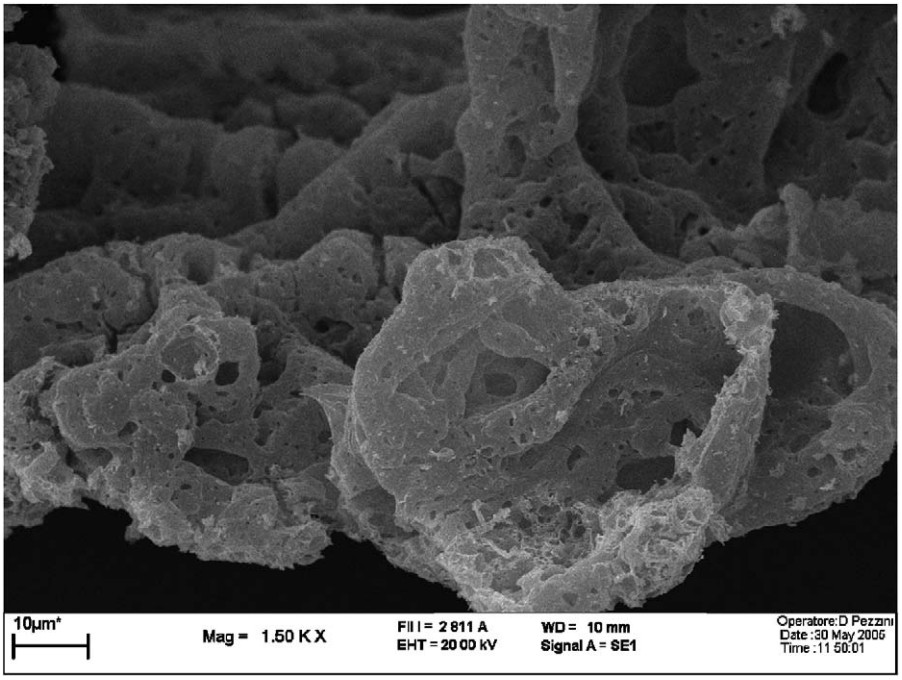

Fig. 3. FESEM view of $CoCr_2O_4$ catalyst crystal agglomerates obtained by combustion synthesis.

Table 1
BET analysis and catalytic activity results

Catalyst	BET ($m^2\ g^{-1}$)	T_{comb} (°C)	T_{red} (°C)	NO conversion at T_{red} (%)
$CoCr_2O_4$	59	396	385	36
Aged $CoCr_2O_4$	39	399	389	29
$MnCr_2O_4$	37	427	331	25
$CoFe_2O_4$	10	446	345	43

mum NO conversion achievable, and the related NO abatement peak temperature (T_{red}) for all of the catalysts investigated. The lower the T_{comb} value, the higher the activity toward soot combustion. Because the main goal of the present investigation was the development of a catalyst for the combined abatement of soot and NO_x, the $CoCr_2O_4$ catalyst was selected for further investigation because it is characterized by the best carbon combustion activity, coupled with significant NO conversion. Despite the fact that the other two catalysts promote NO conversion at lower temperatures, $MnCr_2O_4$ provides the lowest NO abatement yield, and $CoFe_2O_4$ provides the poorest soot combustion activity.

Furthermore, as anticipated from the data given in Table 1, the plots in Fig. 4a show a peculiar feature of the $CoCr_2O_4$ catalyst: the abatement of soot seems to occur simultaneously with the abatement of NO_x. The complete set of products is not reported here for the sake of clarity; it is provided later in Fig. 6. It can be stressed that CO_2 is not the only carbon oxidation product: CO is produced in larger amounts as long as the combustion temperature range of the different catalysts is shifted to higher temperatures. As testified by the lowering of the CO_2 peak areas in Fig. 4, CO_2 selectivity diminishes in the following order: $CoCr_2O_4 > MnCr_2O_4 > CoFe_2O_4 >$ noncatalytic combustion.

Furthermore, explorative TPR runs, performed by feeding fixed beds of the $CoCr_2O_4$ in the absence of carbon (see Fig. 7 later) or with the carbon in the absence of catalyst (see Fig. 5 later), lead to just a small reduction of nitrogen oxides. This confirms that the simultaneous presence of both carbon and catalyst is necessary to enable the desired NO reduction. As described later, NO reduction to N_2 actually occurs only when the simultaneous combustion of soot takes place (see the case of $CoCr_2O_4$ in Fig. 6).

Transient thermal analysis studies (see the oxygen TPD plots in Fig. 4b) were quite helpful in understanding the behavior of the catalysts toward soot oxidation. In line with other studies on perovskite-type catalysts [36,43,44], the superior activity of chromites toward carbon oxidation indeed should result from their significantly higher capacity to deliver active oxygen species compared with that of ferrites. Another key issue is

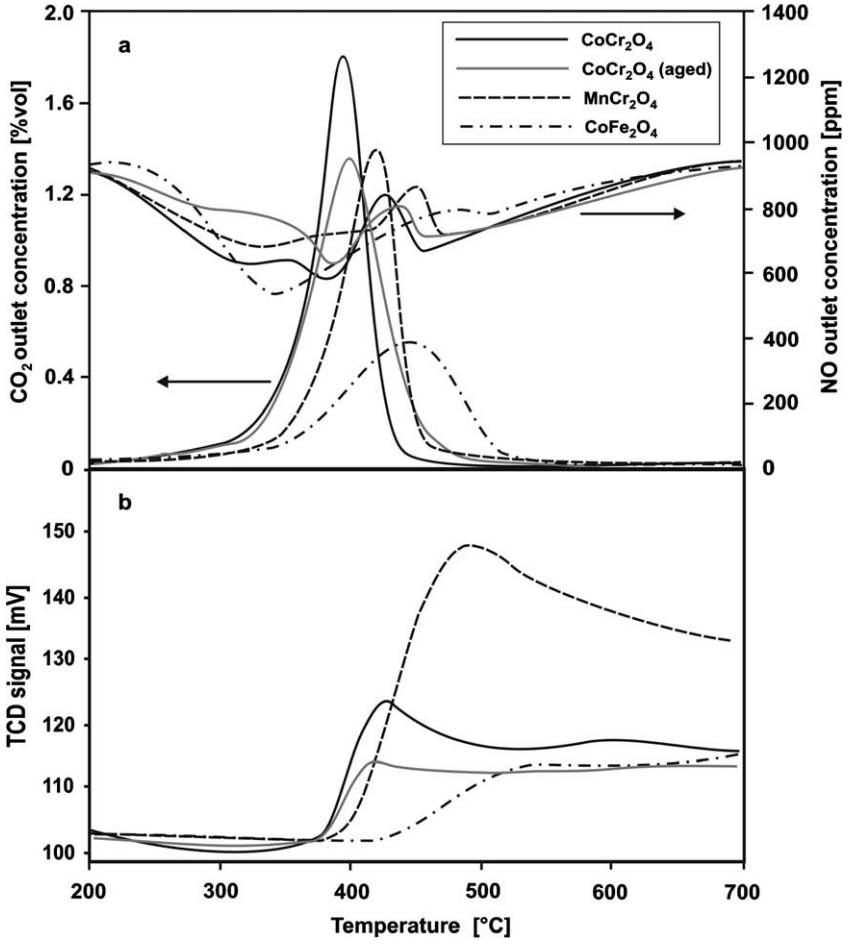

Fig. 4. Results of the TPR (a) (feed concentrations: $O_2 = 10$ vol%, NO = 1000 ppmv, He = balance; catalyst–soot mass ratio = 9:1; catalyst–soot contact conditions = tight; $W/F = 27.1\ kg\,s\,Nm^{-3}$) and oxygen TPD (b) runs performed on the prepared catalysts.

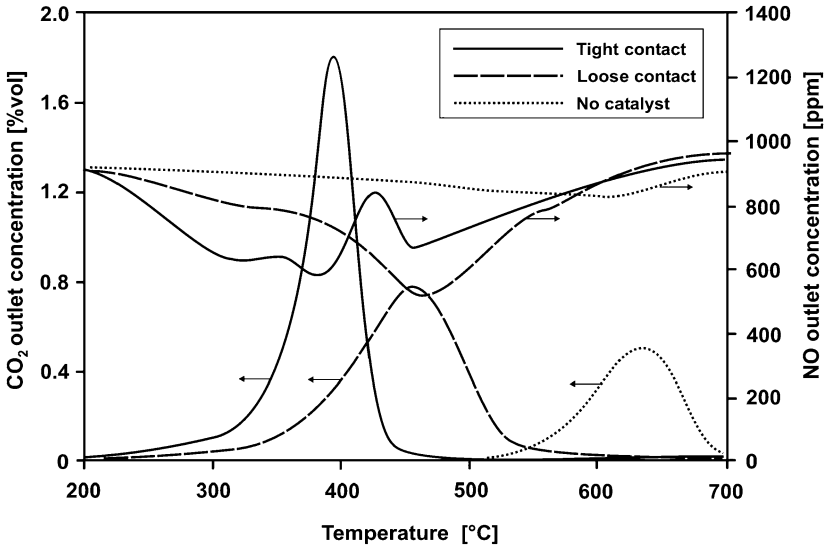

Fig. 5. NO and CO_2 outlet concentration plots obtained during TPR runs performed with the $CoCr_2O_4$ catalyst at different operating conditions (feed composition: 1000 ppmv NO, 10 vol% O_2, He = balance; catalyst–soot mass ratio = 9:1; $W/F = 27.1\ \mathrm{kg\,s\,Nm^{-3}}$).

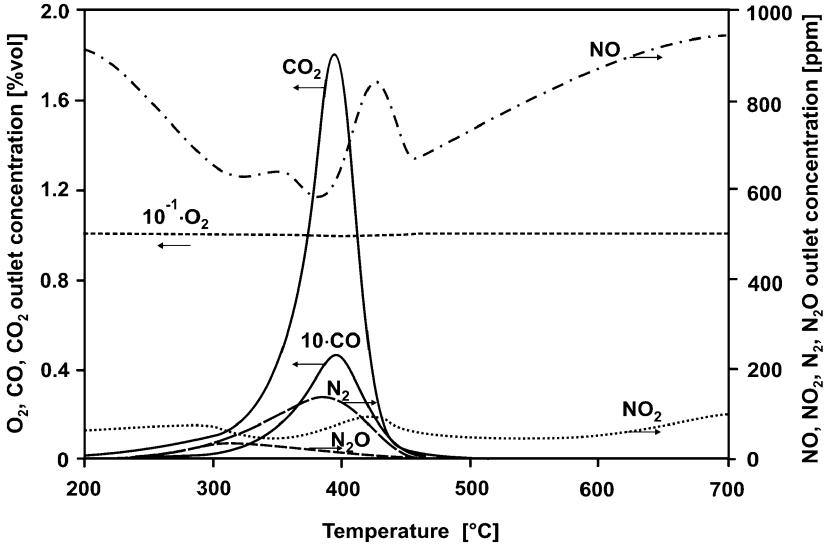

Fig. 6. Concentration plots of the outlet gaseous species in a TPR run performed with the $CoCr_2O_4$ catalyst under tight contact conditions (feed concentrations: O_2 = 10 vol%, NO = 1000 ppmv, He = balance; catalyst–soot mass ratio = 9:1; $W/F = 27.1\ \mathrm{kg\,s\,Nm^{-3}}$).

the temperature at which such oxygen species are desorbed: the lower the temperature, the higher the soot combustion activity. From this standpoint, Fig. 4b provides insight into why the activity order toward soot combustion is $CoCr_2O_4 > MnCr_2O_4 > CoFe_2O_4$. Comparing the plots of the $CoCr_2O_4$ and $MnCr_2O_4$ catalysts suggest that the temperature at which the oxygen species can be released is even more important than the amount of such oxygen species. A certain role should also be played by the SSA (Table 1), which reaches the highest values for the fresh $CoCr_2O_4$ catalyst. However, despite the fact that the aged $CoCr_2O_4$ catalyst exhibits a much lower SSA than the fresh one, it remains more active toward soot combustion than its Mn- or Fe-based counterparts.

By comparing the results of the runs performed under loose or tight contact conditions, Fig. 5 shows how T_{comb} and T_{red} values related to loose contact are some 60–80 °C higher than those related to tight contact. Because most of the runs performed in the present investigation were based on tight contact conditions between catalyst and carbon, the results cannot be considered representative of actual operating conditions in a diesel particulate catalytic trap. In any case, even under loose contact conditions, where the number of contact points between the two catalyst and carbon counterparts is expected to be significantly lower, the catalytic C/NO/O_2 reactions occur significantly faster than for the reference noncatalytic ones (see the dotted lines in Fig. 5).

Fig. 6 shows the complete set of gas outlet concentration plots of the various components involved in a standard TPR run on the $CoCr_2O_4$ catalyst. The scenario is rather complex. CO_2 is by far the main carbon oxidation product, with a selectivity greatly exceeding 95%. CO may play some role as a reducing agent; however, this role should be minor, because NO reduc-

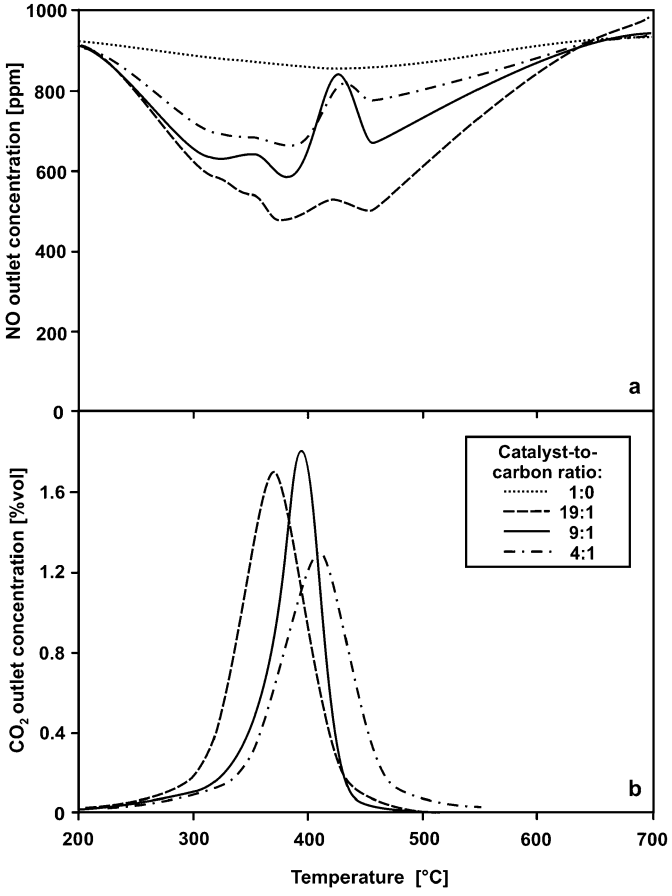

Fig. 7. NO (a) and CO_2 (b) outlet concentration plots obtained during TPR runs performed with the $CoCr_2O_4$ catalyst at different catalyst-to-carbon weight ratios (feed composition: 1000 ppmv NO, 10 vol% O_2, He = balance; catalyst–soot contact conditions = tight).

tion by CO on metal oxide catalysts is known to be strongly inhibited by the presence of oxygen [45], which accounted for 10 vol% of the feed gas mixture in all TPR experiments performed.

The main product of NO reduction is N_2. However, N_2O formation is rather intensive at low temperatures (around 300 °C). Conversely, nitrogen dioxide outlet concentrations, formed to some extent from the fed NO and O_2 according to the $NO + (1/2)O_2 \leftrightarrow NO_2$ equilibrium, generally follows the NO trend. NO_2 should actually contribute to direct carbon combustion, but with a minor effect on N_2 generation, because the main reduction product in this case is NO itself, as mentioned earlier [33].

A particular feature of the NO_x concentration plots becomes apparent as soon as most of the carbon conversion has occurred: NO and NO_2 concentrations are somehow depleted, and a second negative peak can be seen at temperatures around 450 °C, beyond that ascribable to the simultaneous $C/O_2/NO$ reaction occurring below 400 °C. The intensity and the area of this peak seem to be related to the amount of catalyst present, if the curves of Fig. 7 are considered. Furthermore, this second negative peak is not accompanied by the formation of nitrogen or N_2O, as is the first peak. All of these findings indicate that NO and probably NO_2 chemisorption likely occurred, which hampers the possibility to close nitrogen balances among the gaseous molecules. The catalyst acts to some extent as a NO_x storage material. As soon as the temperature exceeded 600–650 °C and no carbon remained to exert a reducing effect, NO/NO_2 desorption occurred, as demonstrated by the increased NO and NO_2 outlet concentration to values even higher than the inlet values. NO chemisorption thus must be considered reversible. Finally, we note that this phenomenon seems to be strictly related to some functional modification of the catalyst surface (e.g., reduction) occurring during the catalyzed combustion of carbon. In fact, the results plotted in Fig. 7 for the TPR run carried out in the absence of carbon show only very limited intrinsic activity of the catalyst toward NO abatement.

The data plotted in Fig. 7 provide the following indications as well:

- The role of the catalyst-to-soot ratio on the catalytic combustion of carbon is positive, as expected. The T_{comb} value becomes lower and lower as the ratio increases (Fig. 7b). This can be attributed mainly to the increased number of contact points between catalyst and carbon at the beginning of each TPR run.
- The absolute value of the negative peak of the NO plot increases with the catalyst-to-soot ratio (Fig. 7a). This is a sign that the $C/O_2/NO$ reaction is simultaneous and similarly influenced by the contact conditions between catalyst and carbon.

If the role of O_2 feed concentration on the studied reaction system is considered, then the following arguments can be put forward based on the data plotted in Fig. 8:

- As the O_2 concentration increases, the catalytic combustion of carbon occurs at lower and lower temperatures; that is, the peak of CO_2 outlet concentration versus temperature becomes narrower and steeper (Fig. 8b). This finding is not surprising, because oxygen is expected to have an evident promoting effect on carbon combustion.
- The occurrence of catalytic combustion even in the absence of oxygen in the feed is conversely quite peculiar. This is should be ascribed to the intrinsic redox activity provided to the catalyst by some of its elements (e.g., Cr, Co). In this case, carbon oxidation is directly related to the reduction of the catalyst itself and is accompanied by a significantly reduced selectivity to CO_2 (down to 35%), with CO as the main product.
- NO reduction occurs simultaneously with carbon combustion independently of the temperature range at which this reaction occurs (Fig. 8a).
- For O_2 inlet concentrations >2 vol%, the shape of the NO outlet concentration peak is roughly comparable to that shown in Figs. 5–7, whereas in the absence of O_2, the NO chemisorption reduction to N_2 (selectivity >95%) becomes extremely intensive. It is very likely that under these conditions, NO chemisorbed species play a nonnegligible role in the carbon oxidation process. Specific runs (not reported here for space considerations) carried out at different NO concentrations and in the absence of oxygen confirm this

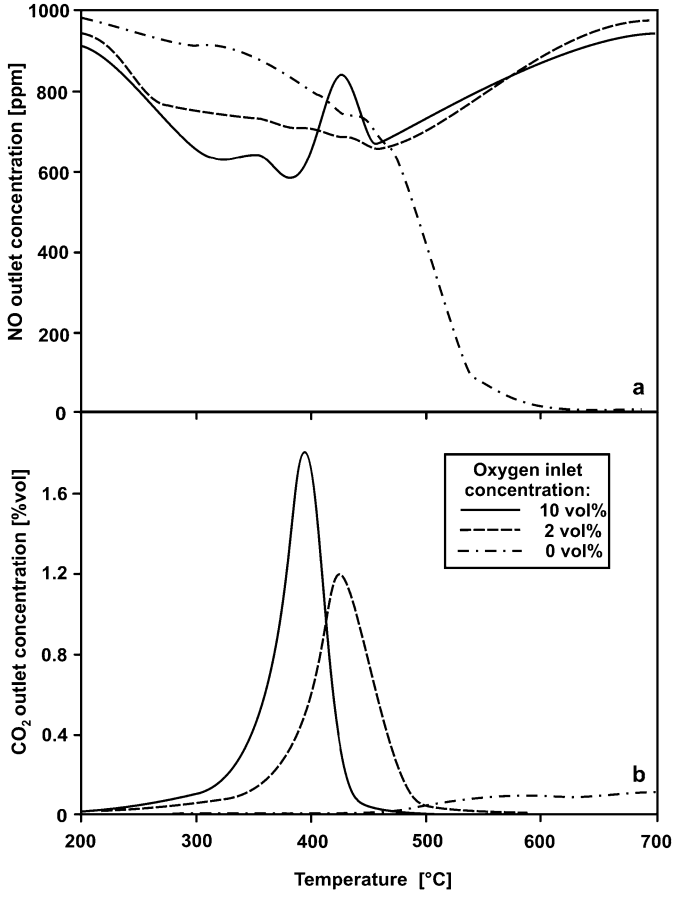

Fig. 8. NO (a) and CO_2 (b) outlet concentration plots obtained during TPR runs performed with the $CoCr_2O_4$ catalyst at different O_2 inlet concentrations (feed composition: 1000 ppmv NO, He = balance; catalyst-to-carbon ratio = 9:1; catalyst–soot contact conditions = tight; $W/F = 27.1\ \mathrm{kg\,s\,Nm^{-3}}$).

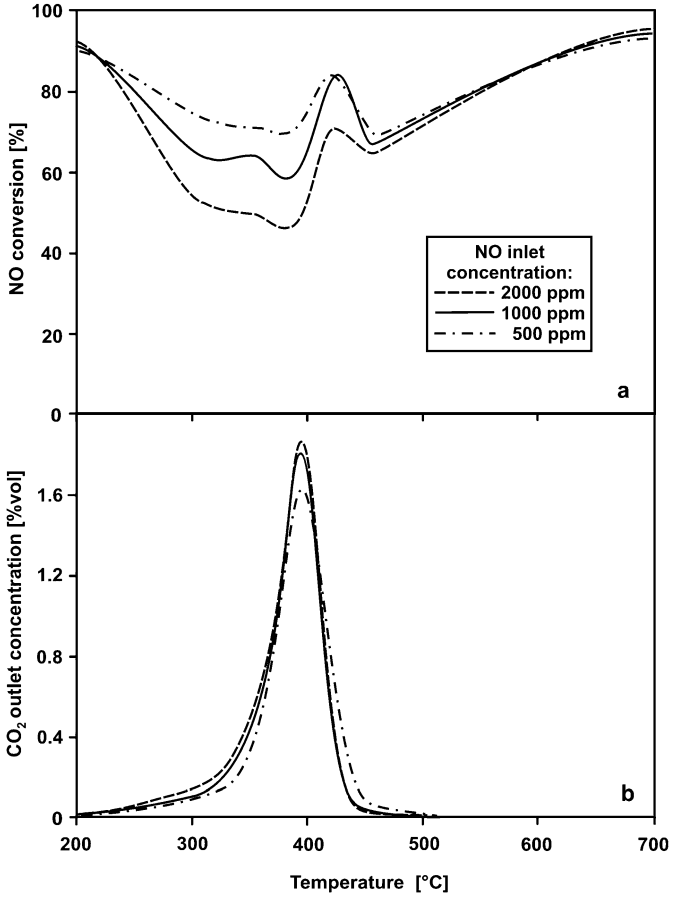

Fig. 9. NO conversion (a) and CO_2 outlet concentration (b) plots obtained during TPR runs performed with the $CoCr_2O_4$ catalyst at different NO inlet concentrations (10 vol% O_2; He = balance; catalyst-to-carbon ratio = 9:1; catalyst–soot contact conditions = tight; $W/F = 27.1\ \mathrm{kg\,s\,Nm^{-3}}$).

hypothesis. It must be stressed, however, that these conditions are unconventional for a lean engine like the diesel one, in which the O_2 concentration in the exhaust ranges from 2% (heavy load) up to 20% (idle).

Finally, the NO conversion plots, shown in Fig. 9 as a function of the inlet NO concentration in TPR runs over the $CoCr_2O_4$ catalyst, are very useful for drawing inference about the NO reaction order in the C/NO/O_2 reaction system. Because the NO percent conversion increases with the inlet NO concentration, such a reaction order should probably be >1. T_{red} remains nearly similar, because it is governed by the simultaneous occurrence of the combustion process, which is not markedly influenced by variations in NO inlet concentration (carbon conversion plots are omitted in Fig. 9 for this reason). This parameter does not significantly affect the temperature range and intensity of the second NO peak, which was previously attributed to NO chemisorption. This should be a sign that this last process should in any case attain saturation of the chemisorption sites created during carbon combustion over the catalyst surface.

On the basis of the experimental evidence described herein, as well as reports in the literature [46–51], the reaction steps listed in Table 2 can be hypothesized. In line with earlier re-

Table 2
Main tentative pathways for the simultaneous reduction of NO and combustion of soot over the $CoCr_2O_4$ catalyst (Legend: O_{ad}, NO_{ad} = oxygen, nitrogen oxide chemisorbed over the catalyst; C_f = active carbon site; $C[i, j] = i, j$ species adsorbed over carbon; g = gas phase)

C/O_2 reaction (adapted from [20])	
$O_2(g) \leftrightarrow 2O_{ad}$	(a)
$C_f + O_{ad} \rightarrow C[O]$	(b)
$C[O] + O_{ad} \rightarrow CO_2(g)(+C_f)$	(c)
$C[O] + (1/2)O_2 \rightarrow CO_2(g)(+C_f)$	(d)
$C[O] \rightarrow CO(g)(+C_f)$	(e)
C/NO/O_2 reaction (adapted from [23–26])	
$NO(g) \leftrightarrow NO_{ad}$	(f)
$C_f + NO_{ad} \rightarrow C[N, O]$	(g)
$C[N, O] + NO_{ad} \rightarrow CO_2(g) + N_2(g)(+C_f)$	(h)
$C[N, O] + NO(g) \rightarrow CO_2(g) + N_2(g)$	(i)
$C[N, O] + NO_{ad}(+C_f) \rightarrow CO_2(g) + C[N, N]$	(j)
$C[N, N] \rightarrow C + N_2(g)$	(k)
$NO(g) + (1/2)O_2 \leftrightarrow NO_2$	(l)
$NO_2(g) \leftrightarrow NO_{ad} + O_{ad}$	(m)
$NO_2(g) + C \rightarrow NO(g) + CO$	(n)
$C[N, N] + O_{ad} \rightarrow N_2O(g) + C$	(o)
$N_2O \rightarrow O_{ad} + N_2$	(p)
$N_2O + O_{ad} \rightarrow O_2 + N_2$	(q)

ports [46,47], the key players in carbon oxidation should be the following ones:

- Oxygen species adsorbed (O_{ad}) on the catalyst surface and obtained by dissociative chemisorption of gas oxygen (reaction (a)).
- Free carbon sites (C_f), particularly active, obtained in the early stages of the combustion process (not considered here) and renewed over the catalyst surface as long as combustion is occurring (see below). These sites can be considered those locations on the carbon surface where an oxidation process has just occurred. A deeper insight into this has been provided previously [48].

The O_{ad} species attack the reactive free carbon (C_f) to give the oxygen-containing active intermediate C[O] over carbon surface (reaction (b)), which in turn produces CO_2 by reacting with either O_{ad} (reaction (c)) or molecular oxygen (reaction (d)), thereby leaving another reactive free carbon species (C_f) available for the reaction processes. Evidence of the presence of such intermediate C[O] species was provided by Kureti et al. [32] using DRIFT spectroscopy. Finally, CO production from the reaction intermediate (reaction (e)) is hypothesized to account for the fact that CO_2 selectivity is high, but not complete.

The active C_f carbon sites are likely to play a crucial role in the simultaneous reduction of NO as well [49,50]. This ties NO reduction to the combustion of carbon, which generates such C_f sites. C[N,O] species over the carbon surface (reaction (g)) by combination of a carbon active site C_f and a NO molecule adsorbed on the catalyst surface, NO_{ad} (reaction (f)). The desired nitrogen formation occurs by reaction of C[N,O] with a further NO_{ad} molecule (reaction (h)) or directly with a gaseous NO molecule (reaction (i)). Evidence of chemisorbed nitrogen oxides on oxide catalysts for diesel soot combustion is not infrequent at the temperatures of interest in the aforementioned reaction [32,35,51]. The FTIR spectra in Fig. 10 for the $CoCr_2O_4$ catalyst show in particular that NO can be easily adsorbed on the catalyst surface, because the absorbance peaks at 1370 and 1395 cm^{-1} can be ascribed to formation of surface nitrites on both Cr and Co sites [52,53] and remain present on the surface of the catalyst at 385 °C (Fig. 10b).

The reaction order >1 versus NO partial pressure can be explained by the fact that this critical step requires the presence of two NO-related species (i.e., NO_{ad}, C[N,O], NO(g)). In line with this, it may also be hypothesized that N_2 may be generated via a further reaction intermediate C[N,N] (reaction (j)), which is then decomposed via reaction (k). Based on the experimental evidence (see Fig. 5), NO_2 formation from NO catalytic oxidation (reaction (l)) and, consequently, its decomposition (reaction (m)) should proceed in a rather limited manner. However, NO_2 should play a certain role in soot combustion according to reaction (n) [33], because its production should be maximized at 300–400 °C as a consequence of kinetic (<300 °C) and thermodynamic limitations (>400 °C) [54].

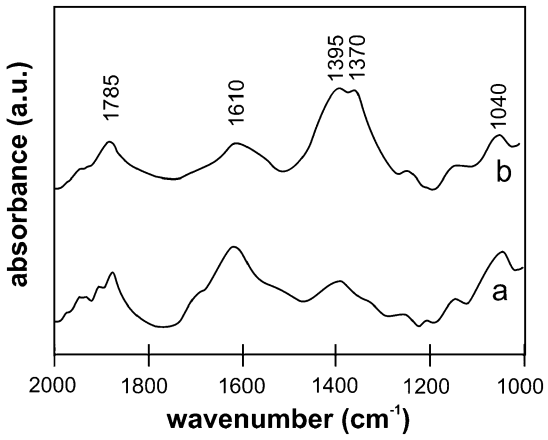

Fig. 10. Transmission FT-IR spectra obtained for the following materials: (a) fresh $CoCr_2O_4$ catalyst, as prepared; (b) catalyst treated at 385 °C under NO flow rate (2000 ppmv) for 60 min and then flushed with He and cooled rapidly by removing it from the oven.

Finally, oxygen could be involved in the formation of N_2O (reaction (o)). In this context, very recent studies [55] have shown that N_2O can be decomposed over spinel catalysts above 350 °C via pathways (p) and (q). This may well be responsible for limiting the overall formation of N_2O to rather low temperatures, as detected experimentally. Deeper insight into the reaction mechanism perhaps may be obtained using a high-temperature spectroscopic technique (e.g., DRIFTS [32,56]) to directly assess the presence of the hypothesised reaction intermediates over the catalyst and carbon surfaces.

4. Conclusions

Some spinel-type catalysts were prepared, characterized, and tested for potential applications in the treatment of diesel exhaust gases as promoters of simultaneous NO_x and soot removal. A typical feature of the most promising catalyst tested ($CoCr_2O_4$) was the simultaneity of NO and soot abatements, occurring at temperatures lower than those enabled by earlier developed perovskite-type catalysts [35]. This success is related in part to the particular synthesis method adopted—solution combustion synthesis, which enables the formation of fine catalyst crystals (<20 nm) and a very foamy structure of their agglomerates. This catalyst microstructure helps in maximizing the number of contact points between catalyst and carbon, a key step in promoting carbon combustion and, consequently, NO reduction.

An experimental test campaign is currently in progress to verify the potential of $CoCr_2O_4$ at a catalytic trap level on actual exhaust gases. Along with this, deeper mechanistic studies are in progress to possibly provide further evidence beyond that given here of the proposed mechanisms for this rather complex solid–solid–gas reaction system.

References

[1] L. Shirnamé-Moré, Diesel Exhaust: A Critical Analysis of Emissions, Exposure, and Health Effects, A Special Report of the Institute's Diesel

Working Group, Health Effects Institute, Cambridge, MA (1995) pp. 221–242.
[2] D.M. Brown, M.R. Wilson, W. MacNee, V. Stone, K. Donaldson, Toxicol. Appl. Pharmacol. 175 (2001) 191.
[3] G. Oberdörster, Z. Sharp, V. Atudorei, A. Elder, R. Gelein, W. Kreyling, C. Cox, Inhal. Toxicol. 16 (2004) 437.
[4] C.M. Somers, B.E. McCarry, F. Malek, J.S. Quinn, Science 304 (2004) 1008.
[5] T. Kawatani, K. Mari, I. Fukano, K. Sugakawa, T. Koyama, Technology for Meeting the 1994 USA, Exhaust Emission Regulations on Heavy-Duty Diesel Engine, SAE Paper No. 932654 (1993).
[6] K. Slodowske, An engine manufacturer's prospective on diesel fuels and the environment, in: Proceedings of the SAE Panel Presentation at SAE Fuels and Lubrificant Meeting, Detroit, 20 October 1993.
[7] H. Hiroyasu, M. Arai, H. Nakanishi, SAE Paper No. 800252 (1980).
[8] A.G. Konstandopoulos, H.J. Johnson, SAE Paper No. 890405 (1989).
[9] D. Fino, N. Russo, C. Badini, G. Saracco, V. Specchia, AIChE J. 49 (2003) 2173.
[10] P. Marecot, A. Fackhe, L. Pirault, C. Geron, G. Mabilon, M. Prigent, J. Barbies, Appl. Catal. B 5 (1994) 57.
[11] C.L. Liang, K.J. Baumgard, R.A. Gorse, J.E. Orban, J.M.E. Storey, J.C. Tan, J.E. Thoss, W. Clark, SAE Paper No. 2000-01-1876 (2000).
[12] J.M. Valentine, J.D. Peter-Hoblyn, G.K. Acres, SAE Paper No. 2000-01-1934 (2000).
[13] P. Hawker, N. Myers, V.H.Th. Hüthwohl, B. Bates, L. Magnusson, P. Bronnenberg, SAE Paper No. 970182 (1997).
[14] P. Kojetin, F. Janezich, L. Sura, D. Tuma, SAE Paper No. 930129 (1993).
[15] H. Houben, R. Miebach, J.E. Sauerteich, SAE Paper No. 942264 (1994).
[16] M. Gautam, S. Popuri, B. Rankin, M. Seehra, SAE Paper No. 1999-01-3565 (1999).
[17] B.A.A.L. Van Setten, M. Makkee, J.A. Moulijn, Catal. Rev.-Sci. Eng. 43 (2001) 489.
[18] M. Makkee, H.C. Krijnsen, S.S. Bertin, H.P.A. Calis, C.M. van den Bleek, J.A. Moulijn, Catal. Today 75 (2002) 459.
[19] C.Y. Lee, K.Y. Chai, B.H. Ha, Appl. Catal. Part B Environ. 5 (1994) 7.
[20] K. Yoshida, S. Makino, S. Sumiya, G. Muramatsu, R. Helferich, SAE Paper No. 892046 (1989).
[21] F. Kapteijn, A.J.C. Mierop, G. Abbel, J.A. Moulijn, J. Chem. Soc. Chem. Commun. 16 (1984) 1085.
[22] N. Kakuta, S. Sumiya, K. Yoshida, Catal. Lett. 11 (1991) 71.
[23] K. Matsuoka, H. Orikasa, Y. Itoh, P. Chambrion, A. Tomita, Appl. Catal. B 26 (2000) 89.
[24] Y. Teraoka, K. Nakano, S. Kagawa, W.F. Shangguan, Appl. Catal. B 5 (1995) L181.
[25] W.F. Shangguan, Y. Teraoka, S. Kagawa, Appl. Catal. B 8 (1996) 217.
[26] Y. Teraoka, K. Nakano, W.F. Shangguan, S. Kagawa, Catal. Today 27 (1996) 107.
[27] W.F. Shangguan, Y. Teraoka, S. Kagawa, Appl. Catal. B 12 (1997) 237.
[28] W.F. Shangguan, Y. Teraoka, S. Kagawa, Appl. Catal. B 16 (1998) 149.
[29] Y. Teraoka, K. Kanada, S. Kagawa, Appl. Catal. B 34 (2001) 73.
[30] S. Xiao, K. Ma, X. Tang, H. Shaw, R. Pfeffer, J.G. Stevens, Appl. Catal. B 32 (2001) 107.
[31] W. Weisweiler, K. Hizbullah, S. Kureti, Chem. Eng. Technol. 25 (2002) 140.
[32] S. Kureti, W. Weisweiler, K. Hizbullah, Appl. Catal. B 43 (2003) 281.
[33] B.J. Cooper, J.E. Thoss, SAE Paper No. 890404 (1989).
[34] R. Allanson, B.J. Cooper, J.E. Thoss, A. Uusimäki, A.P. Walker, J.P. Warren, SAE Paper No. 2000-01-0480 (2000).
[35] D. Fino, P. Fino, G. Saracco, V. Specchia, Appl. Catal. B 43 (2003) 243.
[36] A. Civera, M. Pavese, G. Saracco, V. Specchia, Catal. Today 83 (2003) 199.
[37] N. Russo, D. Fino, G. Saracco, V. Specchia, J. Catal. 229 (2005) 459.
[38] D. Fino, N. Russo, G. Saracco, V. Specchia, Chem. Eng. Sci. 59 (2004) 5329.
[39] A. Yezerets, N.W. Currier, H.A. Eadler, A. Suresh, P.F. Madden, M.A. Branigin, Catal. Today 88 (2003) 17.
[40] A. Yezerets, N.W. Currier, D.H. Kim, H.A. Eadler, W.S. Epling, C.H.F. Peden, Appl. Catal. B Environ. 61 (2005) 120.
[41] M. Ambrogio, G. Saracco, V. Specchia, C. van Gulijk, M. Makkee, J.A. Moulijn, Sep. Purif. Technol. 27 (2002) 195.
[42] D. Fino, P. Fino, G. Saracco, V. Specchia, Chem. Eng. Sci. 58 (2003) 951.
[43] D. Fino, N. Russo, G. Saracco, V. Specchia, J. Catal. 217 (2003) 367.
[44] L. Forni, I. Rossetti, Appl. Catal. B 38 (2002) 29.
[45] B. Viswanathan, Catal. Rev.-Sci. Eng. 34 (1992) 337.
[46] A.F. Ahlström, C.U.I. Odenbrand, Appl. Catal. 60 (1990) 143.
[47] A.F. Ahlström, C.U.I. Odenbrand, Appl. Catal. 60 (1990) 157.
[48] B.R. Stanmore, J.F. Brilhac, P. Gilot, Carbon 39 (2001) 2247.
[49] Y. Teraoka, W.F. Shangguan, K. Jansson, M. Nygren, S. Kagawa, Bull. Chem. Soc. Jpn. 72 (1999) 133.
[50] W.F. Shangguan, Y. Teraoka, S. Kagawa, Appl. Catal. B Environ. 12 (1997) 237.
[51] A.L. Goodman, E.T. Bernard, V.H. Grassian, J. Phys. Chem. 88 (2001) 6443.
[52] J. Laane, J.R. Ohlsen, Prog. Inorg. Chem. 27 (1980) 465.
[53] FDM FTIR Spectra of Minerals and Inorganic Compounds, Copyright© 1997, Fiveash Data Management, Inc. http://www.fdmspectra.com/.
[54] J. Despres, M. Koebel, M. Elsener, A. Wokaun, PSI Scientific Rep. 2001 5 (2002) 64.
[55] N. Russo, D. Fino, G. Saracco, V. Specchia, Catal. Today, in press.
[56] G. Mul, F. Kapteijn, J.A. Moulijn, Carbon 37 (1999) 401.